

Polarization-analyzing CMOS image sensor with embedded wire-grid polarizers

Takashi Tokuda, Hirofumi Yamada, Hiroya Shimohata, Kiyotaka, Sasagawa, and Jun Ohta

Graduate School of Materials Science, Nara Institute of Science and Technology,
8916-5 Takayama, Ikoma, Nara, 630-0192, JAPAN

tokuda@ms.naist.jp

TEL: +81-743-72-6050, FAX: +81-743-72-6059

1. Introduction

In this work, a polarization-analyzing CMOS sensor based on image sensor architecture was proposed and demonstrated. The sensor has a feature of monolithically embedded polarizer. We designed a prototype sensor equipped with a polarization-analyzing pixel array based on the concept. Embedded polarizers with different angle were implemented to realize a real-time absolute measurement of incident polarization angle. We characterized the functionality and performance of the designed polarization-analyzing CMOS image sensor. We also experimentally performed polarimetric measurements of chiral solution with the fabricated sensor.

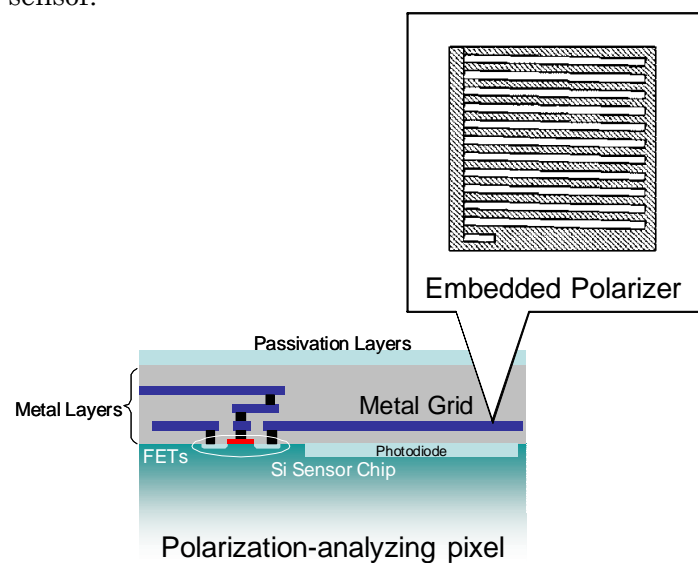


TABLE I: Specifications of the polarization-analyzing CMOS image sensor

Process	0.35 μm 2 poly 4 metal standard CMOS
On-chip Polarizer	Line/Space = 0.6 μm /0.6 μm (1.2 μm pitch)
Pixel size	20 μm \times 20 μm
Photodiode size	10 μm \times 10 μm (Fill factor: 25%)
Array size	30 \times 30 (15 \times 15 pixel sets (see Fig. 4))
Operating Voltage	3.3 V
Chip size	1880 μm \times 1880 μm
Readout	Analog Voltage, 4 channel

Fig. 1: Concept of the polarization-analyzing CMOS image sensor

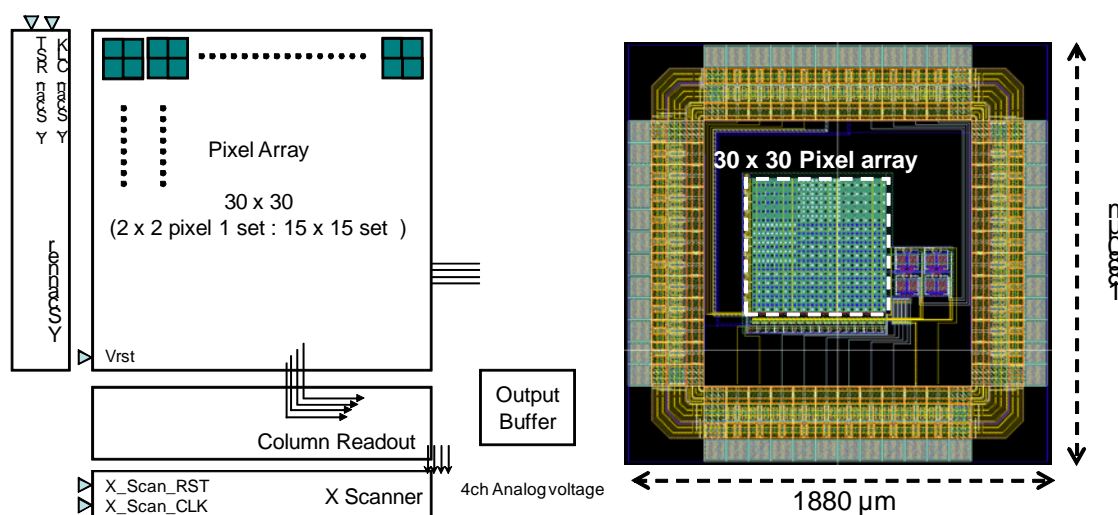


Fig. 2: (a) Block diagram and (b) layout of the polarization-analyzing CMOS image sensor

2. Concept and design of the polarization-analyzing CMOS image sensor

Fig. 1 shows the concept of the polarization-analyzing CMOS image sensor. The sensor has features of:

- (1) Each pixel has polarization dependent sensitivity.
- (2) The pixel array consists of pixels with different polarizer angle.

Based on this concept, we have designed a polarization analyzing CMOS image sensor using 0.35 μm 2 poly 4 metal standard CMOS technology. Fig. 2 shows block diagram and layout of the sensor, and Table I

shows the specifications of the sensor. From the viewpoint of the circuitry, the sensor is a conventional 3 transistor active pixel sensor (APS). As shown in Fig. 3, the pixel was designed in 2 x 2 pixel set. We took this configuration to realize analytical schemes of (1) intensity normalization and (2) differential detection between adjacent pixels simultaneously. The four pixels in the pixel set are accessed, and the light intensities obtained by the four pixels are read out simultaneously to compare and normalize each other. Corresponding to the 2 × 2 pixel set configuration, the columnar readout circuit is implemented parallel and in four channels. The size of the pixel is 20μm x 20μm for one pixel and the size of the photodiode is 10 μm x 10 μm. Fill factor is 25 %. The photodiode was designed with n-well/p-sub structure. We configured different polarizer structure in the 2 x 2 pixel set. On pixel A and B, we configured the same polarizer structure in θ , and $\theta+90\text{deg}$. We took this configuration to make the sensor compatible with the $\theta+45^\circ$ detection scheme used in the previous work [2].

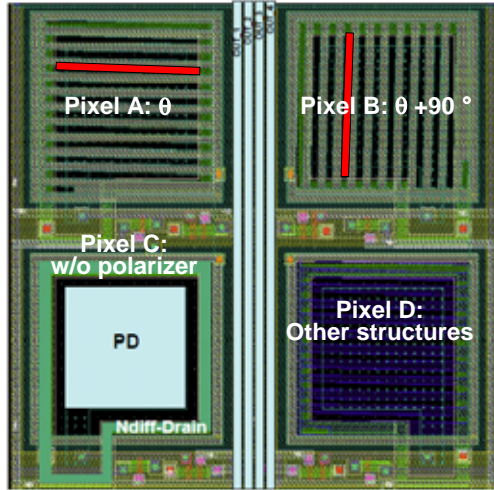


Fig. 3: Layout of the 2 x 2 pixel set with embedded polarizers

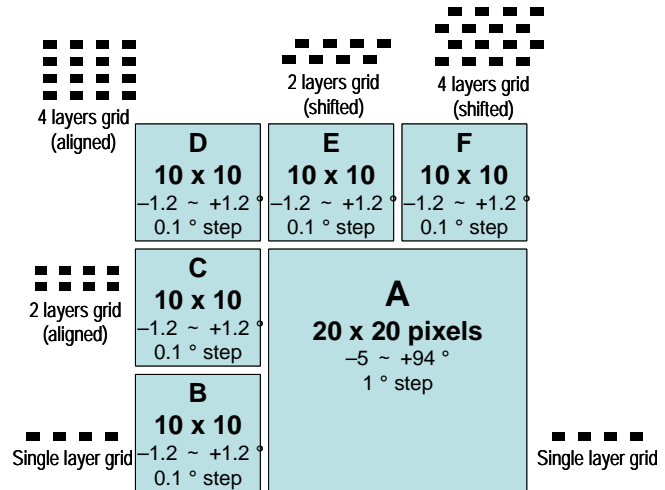


Fig. 4: Configuration of the pixel array

The pixel array of the sensor has 30 × 30 pixels (15 × 15 pixel sets). The pixel sets could be divided into one 10 × 10 array and five 5 × 5 arrays. Fig. 4 shows the configuration of the partial pixel arrays. The partial pixel arrays are denoted as A to F. The features of each partial pixel array are shown in Fig. 4, too. The partial pixel arrays A to F were designed to demonstrate and characterize the following functions.

- 1) A (10 × 10 pixel sets) was designed with θ ranging from -5° to 94° . This partial pixel array was designed to realize the main objective of the sensor: the real-time absolute measurement of the incident polarization angle.
- 2) B to F (5 × 5 pixel sets) were designed with θ ranging from -0.12° to 0.12° . These arrays were designed to explore the possibility of improving the performance of the embedded polarizer with a stacked wire grid structure. The embedded polarizers implemented on the partial pixel arrays B to F have different layer structures, as shown in Fig. 4.

3. Functional characterization of the polarization-analyzing CMOS image sensor

Basic performances of the fabricated sensor are shown in TABLE II. The interframe random noise was 0.64 LSB_{rms} (without interframe averaging). The noise level was decreased to as less as 0.33 LSB_{rms} with an interframe averaging (10 frames or more).

Performance of the polarization-analyzing pixel was evaluated by measuring the polarization-dependent sensitivity of the pixels. The sensor was illuminated with monochrome linearly polarized light. The polarization angle of the incident light was varied from 0 to 180 deg. Fig. 5 shows typical polarization profile of the normalized pixel value, which represents the transmittance of the on-chip embedded polarizer. In Fig. 4, the horizontal axis (Polarization angle) represents the angle of the electric vector of incident light to the embedded polarizer grid. The transmittance of the embedded polarizer becomes maxima when the electric vector is parallel to the grid structure. It is in an opposite situation from wire grid polarizes used in the wavelength region larger than grid pitch [3]. We performed electromagnetic simulation to understand the crossover of the transmittance in the short wavelength region.

In this work, the ratio of the maximum to minimum normalized intensity in the angular profile, named the extinction ratio, was used to evaluate the performance of the polarizer. The extinction ratio obtained with the single-layer embedded polarizer was 2.03, as shown in Fig. 5. This value was smaller than that for other conventional polarizers such as the Glan-Thompson prism. This small extinction ratio is also due to the fact that the wavelength was comparable in size to the grid pitch.

TABLE II: Basic performances of the sensor circuitry

Performance	Result	Note
Random noise [LSBrms]	0.64	Dark, no averaging
Fixed pattern noise [LSBrms]	14.1	Raw data
(10 interframe averaging)	0.46	After offset subtraction
Transfer gain [mV/LSB]	1.38	PD level to digitized value
Available output range [LSB]	1278	Corresponding to 1.8 V discharge

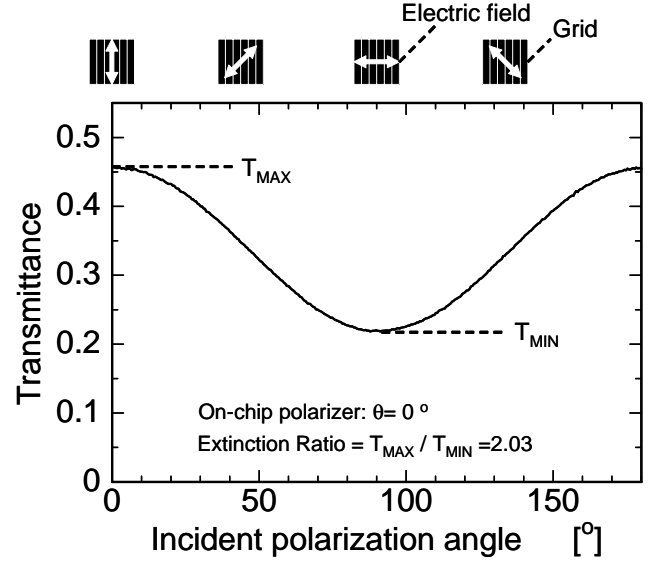


Fig. 5: Typical single-pixel polarization profile

The pixels with stacked polarizers were also characterized. However, in the present design, we did not obtain significant improvement in the performance of the stacked polarizers. More detailed electromagnetic consideration and simulation is required to take advantage of stacking structures.

Since the pixel-level performance was revealed to be limited as shown in Fig. 5, we developed an estimation scheme based on the values obtained with 180 pixels with different polarizer angles. When the sensor was illuminated with a uniform and linearly polarized light with a polarization angle of φ , the normalized pixel value T_θ (transmittance of the embedded polarizer) showed a sinusoidal dependence on the polarizer angle θ as follows:

$$T_\theta = A \cos(2\theta - 2\varphi) + B \quad (1)$$

where A and B are constants. The phase of the polarization profile plotted to 2θ can be interpreted as the incident polarization angle 2φ . Since the period of the profile was known to be 180° , φ could be estimated on the basis of the Fourier transform as follows:

$$2\varphi = \tan^{-1} \frac{\sum_{n=0}^{179} T_n \cdot \sin(2n)}{\sum_{n=0}^{179} T_n \cdot \cos(2n)} \quad (2)$$

To evaluate the performance of the estimation schemes, the sensor was illuminated with various polarization angles φ between 0° and 90° ; the estimated polarization angle was then recorded.

Fig. 6 shows the experimentally obtained angular error profile of the full-angle estimation scheme. As shown in Fig. 6, the noise level was as large as 0.04 deg. and angular error was less than 1 deg. The angular errors were static and noise level is one order smaller than the static angular error. We can omit the static angular error using simple compensation based on the measured profile such as Fig. 6. Thus, the accuracy of the estimation is limited only by the noise level.

It is interesting to note that the measurement accuracy of 0.04° was available when using the embedded polarizer configured with a 1° step.

4. Functional demonstration in polarimetric measurement of chiral solution

Polarimetric measurements were performed to demonstrate the applicability of the present polarization-analyzing CMOS image sensor for chiral measurement. A quartz cell filled with sucrose solution was inserted into the light path. The change in the estimated polarization angle caused by the insertion of the sample cell was the optical rotation of the sample solution. The concentration of sucrose solution varied from 0.001 to 0.256 g/ml in a logarithmic manner.

Fig. 7 shows the optical rotations of sucrose solutions measured by the present sensor. The rotation angle was successfully measured, as expected from the results of Fig. 6. The minimum detectable concentration was 0.008 g/ml with the full-angle estimation scheme. This measurement limit was as good as the best results obtained with the differential measurements of the optical rotation using variable incident polarization requiring a highly accurate rotating polarizer system [2]. The present sensor architecture based on a CMOS image sensor proved to be feasible for chiral analysis with a fixed incident polarization.

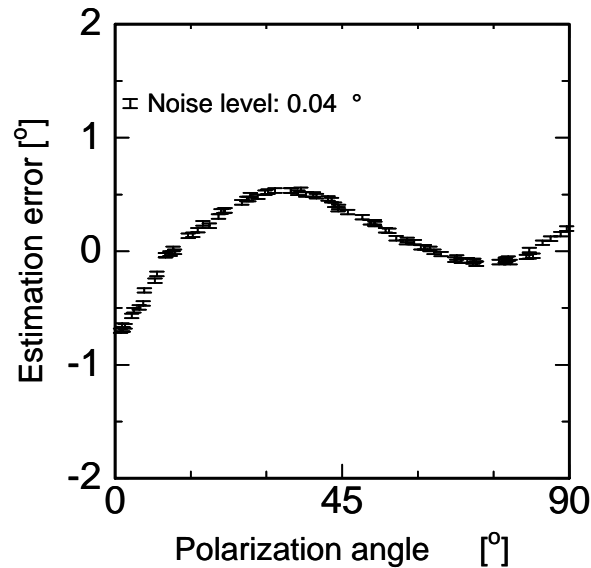


Fig. 6: Estimation performance (error profile) obtained with the full-angle estimation scheme

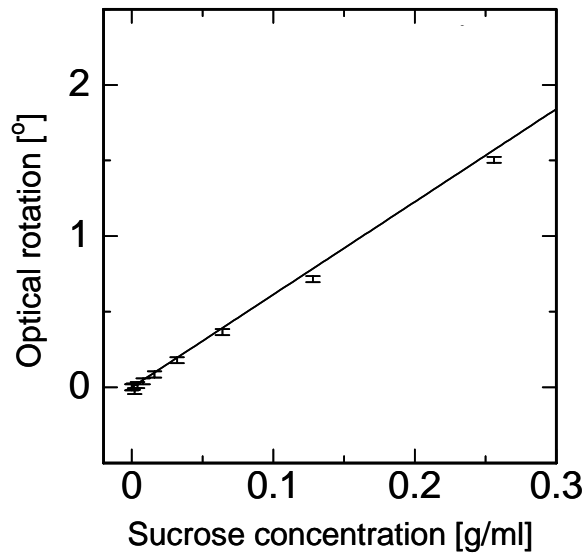


Fig. 7: Result of polarimetric measurement of chiral solution (sucrose solution)

5. Conclusions

A polarization-analyzing CMOS image sensor was proposed and designed with $0.35\ \mu\text{m}$ 2 poly 4 metals standard CMOS technology. The sensor has a feature of monolithically embedded polarizer. The angle of the embedded polarizer was varied to realize a real-time absolute measurement of incident polarization angle. Although the extinction ratio of the embedded polarizer was as small as 2, we demonstrated that estimation schemes based on the variation of the polarizer angle provide an accuracy of $0.04\ \text{deg}$. This accuracy was also confirmed in polarimetric measurements of the chiral solution.

Acknowledgements

This work was supported by Grant-in-Aid #21310081 for Scientific Research from the Ministry of Education, Culture, Sports, Science and Technology of Japan. This work was also supported by the VLSI Design and Education Center (VDEC), University of Tokyo, in collaboration with Cadence Design Systems, Inc.

References

- [1] Z. Y. Yang, and Y. F. Lu, "Broadband nanowire-grid polarizers in ultraviolet-visible-near-infrared regions," *Optics Express*, 15, pp. 9510-9519., 2007.
- [2] T. Tokuda, S. Sato, H. Yamada, K. Sasagawa, and J. Ohta, "Polarization-analyzing CMOS photosensor with monolithically embedded wire grid polarizer," *Electronics Letters*, 45, 228(2009)
- [3] J. Raynor, "Polarization sensitive solid state image sensor including integrated photodetector and polarizing assembly and associated methods." US patent 7186968, March 2007.

